BBA - Bioenergetics 1860 (2019) 724–733

Contents lists available at ScienceDirect

BBA - Bioenergetics

journal homepage: www.elsevier.com/locate/bbabio

The human uncoupling proteins 5 and 6 (UCP5/SLC25A14 and UCP6/SLC25A30) transport sulfur oxyanions, phosphate and dicarboxylates

Ruggiero Gorgoglione[a,1], Vito Porcelli[a,1], Antonella Santoro[a,1], Lucia Daddabbo[a], Angelo Vozza[a,b], Magnus Monné[a,c], Maria Antonietta Di Noia[a], Luigi Palmieri[a,b,d], Giuseppe Fiermonte[a,b,*], Ferdinando Palmieri[a,b,d]

[a] Department of Biosciences, Biotechnologies and Biopharmaceutics, Laboratory of Biochemistry and Molecular Biology, University of Bari Aldo Moro, Via E. Orabona 4, 70125 Bari, Italy
[b] Center of Excellence in Comparative Genomics, University of Bari, via Orabona 4, 70125 Bari, Italy
[c] Department of Sciences, University of Basilicata, Via Ateneo Lucano 10, 85100 Potenza, Italy
[d] CNR Institute of Biomembranes, Bioenergetics and Molecular Biotechnologies (IBIOM), 70126 Bari, Italy

ARTICLE INFO

Keywords:
Hydrogen sulfide
Membrane transport
Mitochondria
Mitochondrial carrier
UCP5
UCP6

ABSTRACT

The human genome encodes 53 members of the solute carrier family 25 (SLC25), also called the mitochondrial carrier family. In this work, two members of this family, UCP5 (BMCP1, brain mitochondrial carrier protein 1 encoded by *SLC25A14*) and UCP6 (KMCP1, kidney mitochondrial carrier protein 1 encoded by *SLC25A30*) have been thoroughly characterized biochemically. They were overexpressed in bacteria, purified and reconstituted in phospholipid vesicles. Their transport properties and kinetic parameters demonstrate that UCP5 and UCP6 transport inorganic anions (sulfate, sulfite, thiosulfate and phosphate) and, to a lesser extent, a variety of dicarboxylates (e.g. malonate, malate and citramalate) and, even more so, aspartate and (only UCP5) glutamate and tricarboxylates. Both carriers catalyzed a fast counter-exchange transport and a very low uniport of substrates. Transport was saturable and inhibited by mercurials and other mitochondrial carrier inhibitors at various degrees. The transport affinities of UCP5 and UCP6 were higher for sulfate and thiosulfate than for any other substrate, whereas the specific activity of UCP5 was much higher than that of UCP6. It is proposed that a main physiological role of UCP5 and UCP6 is to catalyze the export of sulfite and thiosulfate (the H_2S degradation products) from the mitochondria, thereby modulating the level of the important signal molecule H_2S.

1. Introduction

Besides playing a central role in respiration and cellular energy supply, mitochondria are involved in a variety of metabolic pathways and cell functions. Because individual steps in these processes are carried out in different cellular compartments, a continuous and highly diversified flux of metabolites, nucleotides and cofactors takes place across the inner mitochondrial membrane. Both the import of solutes produced outside the mitochondria and the export of some formed inside the mitochondrial matrix are accomplished, mainly but not exclusively, by a superfamily of transporters known as the mitochondrial carrier family (MCF) or the SLC25 protein family [1–3]. Family members can be recognized easily by their striking sequence features. Their primary structure consists of three tandemly repeated 100 residue domains, and each domain contains two hydrophobic segments and a signature sequence motif PX[D/E]XX[K/R]X[K/R] (20–30 residues) [D/E]GXXXX[W/Y/F][K/R]G (PROSITE PS50920, PFAM PF00153 and IPR00193) [4]. MCs are wide spread in eukaryotes; *Homo sapiens* has 53 members, *Saccharomyces cerevisiae* 35 and *Arabidopsis thaliana* 58 [5]. Although a considerable number of these carriers have been identified and characterized in terms of substrate specificity, transport properties and kinetic parameters by direct transport assays [6], many other MCs remain to be characterized.

The mammalian uncoupling protein 1 (UCP1) was shown to

Abbreviations: AtUCP, *Arabidopsis thaliana* uncoupling protein; DIC, dicarboxylate carrier; hUCP, *Homo sapiens* uncoupling protein; MC, mitochondrial carrier; MCF, mitochondrial carrier family; OGC, 2-oxoglutarate carrier; Pi, phosphate; ROS, reactive oxygen species

* Corresponding author at: Department of Biosciences, Biotechnologies and Biopharmaceutics, University of Bari, Via E. Orabona 4, 70125 Bari, Italy, 0039-0805442789.
E-mail address: giuseppe.fiermonte@uniba.it (G. Fiermonte).
[1] These authors contributed equally to this work.

https://doi.org/10.1016/j.bbabio.2019.07.010
Received 3 May 2019; Received in revised form 27 June 2019; Accepted 25 July 2019
Available online 26 July 2019

transport protons, thereby uncoupling oxidative phosphorylation, and play a crucial role in non-shivering thermogenesis [7,8]. Based on their homology with UCP1, six members of the MCF in both humans (hUCP1-6) and Arabidopsis (AtUCP1-6) were classified as putative "uncoupling proteins". Indeed, in several publications UCPs 2 to 5 were shown to display uncoupling effects [9–15], but not UCP6 [16]. However, the discovery of UCP homologs in several ectothermic species questioned the role of these proteins in thermogenic processes. Later AtUCP4-6 were demonstrated to be dicarboxylate carriers (AtDIC1-3) [17], hUCP2 was found to be a four-carbon metabolite/P_i carrier [18], and more recently AtUCP1 and AtUCP2 have been shown to be transporters of aspartate, glutamate and dicarboxylates [19].

In the present study, we have investigated the transport properties of two other human UCPs, i.e. UCP5, also known as BMCP1 (brain mitochondrial carrier protein 1) and UCP6, also known as KMCP1 (kidney mitochondrial carrier protein 1) [9,16]. These proteins are encoded by *SLC25A14* and *SLC25A30*, are 325 and 291 amino acids long, respectively, and are highly homologous (72% identical amino acids and 79% similarity). Previously, UCP5 was shown to be localized in mitochondria and to be predominantly expressed in brain, in both neurones and astrocytes, where it is the most abundant UCP [9,15,20–22]. There are three isoforms of UCP5: a 325 amino acid "long" isoform (UCP5L), a 322 amino acid "short" isoform (UCP5S), that lacks the tripeptide VSG at position 23–25 of UCP5L, and an isoform (UCP5SI) containing a 31-amino acid insertion between Arg_{195} and Gly_{196} of UCP5S before the fourth transmembrane α-helix [20]. UCP6 is also localized to mitochondria and almost exclusively expressed in the proximal and distal tubules of kidney cortex [16]. The results presented here demonstrate that UCP5 and UCP6 are mitochondrial transporters for a variety of metabolites with a preference for sulfate and thiosulfate. A primary function of UCP5 and UCP6 is to catalyze the export of the H_2S degradation products from the mitochondrial matrix of mainly brain and kidney, respectively, thereby modulating the level of the important signal molecule H_2S.

2. Materials and methods

2.1. Sequence analysis

BLAST and reciprocal BLAST were used to search for homologs of human UCP5 and UCP6 in e!Ensamble and UniProt. Sequences were aligned with ClustalW. PhyML v3.1 was used to create the phylogenetic tree of uncoupling proteins and their homologs from a multiple-sequence alignment with Muscle in Seaview4.

2.2. Construction of the expression plasmids and mutagenesis

The coding sequences for UCP5L and UCP5S (NM_001282195 and NM_001282196, respectively) and UCP6 (NM_001010875) were amplified by PCR from human brain cDNA library and human kidney cDNA library, respectively. The forward and reverse primers were synthesized corresponding to the extremities of the coding sequences with additional *Nde*I and *Eco*RI (for UCP5L and UCP5S) or *Nde*I and *Bam*HI (for UCP6) restriction sites as linkers. The amplified products were cloned into pRUN (UCP5L and UCP5S) and pMW7 (UCP6) expression vectors. Furthermore, to improve the expression in *Escherichia coli* of UCP6, the sequence 5′-GGTATCTTTCCCGGA-3′ (corresponding to codons 2-6 of the *SLC25A14* gene encoding UCP5L) was introduced between codons 1 and 2 of the UCP6 coding sequence, cloned in the pMW7 vector, by using the QuikChange Site-Directed Mutagenesis Kit (Stratagene). All the constructs were transformed into *E. coli* TOP 10 cells (Invitrogen). Transformants were selected on LB plates containing ampicillin (100 μg/ml) and screened by direct colony PCR and restriction digestion of plasmids. The sequences of the inserts were verified by sequencing.

2.3. Bacterial expression and purification of recombinant proteins

The expression of UCP5L, UCP5S and UCP6 as inclusion bodies in the cytosol of *E. coli* was accomplished as described previously [23–25], except that the host cells were *E. coli CO214*(DE3). Control cultures with the empty vectors were processed in parallel. The inclusion bodies were purified on a sucrose density gradient, washed at 4 °C first with TE buffer (10 mM Tris-HCl and 1 mM EDTA, pH 7.0), then twice with a buffer containing 3% (*w/v*) Triton X-114, 1 mM EDTA, 20 mM Na_2SO_4 and 10 mM MOPS-NaOH, pH 7, and last twice with TE buffer [26,27]. Finally, UCP5L, UCP5S and UCP6 were solubilized in 1.7% (w/v) dodecanoylsarcosine (sarkosyl) [23,28,29], and small residues of unsolubilized material were removed by centrifugation (20,800 × *g* for 15 min at 4 °C).

2.4. Reconstitution of the UCP5L, UCP5S and UCP6 into liposomes

The solubilized recombinant proteins were reconstituted into liposomes by cyclic removal of the detergent with a hydrophobic column of Amberlite beads, as described previously [30] with some modifications. The composition of the initial mixture used for reconstitution was: 20 μl of purified protein (approx. 1.5 μg for UCP5L and UCP5S and 3.0 μg for UCP6), 75 μl of 10% Triton X-114, 85 μl of 10% phospholipids (L-α-phosphatidylcholine from dried egg yolk, Sigma-Aldrich Cat. #61771) in the form of sonicated liposomes [31], 20 mM sodium sulfate (except where otherwise indicated), 1.14 mM EDTA, 0.4 mg of cardiolipin (a mitochondrial inner membrane lipid, which is required for the function of many MCs [32–34]), 20 mM MES/20 mM MOPS at pH 6.0 (except where otherwise indicated) and water to a final volume of 700 μl. After vortexing, this mixture was recycled 14 times through an Amberlite (Bio-Beads SM-2, Biorad Cat. #152-3920) (to remove the detergent) column pre-equilibrated with a buffer containing 20 mM MES/MOPS (pH 6.0) and the substrate at the same concentration as in the starting mixture. All operations were performed at 4 °C, except the passages through Amberlite, which were carried out at room temperature.

2.5. Transport assays

External substrate was removed from proteoliposomes on Sephadex G-75 columns pre-equilibrated with a buffer containing 50 mM NaCl and 20 mM MES/MOPS pH 6.0 (except where otherwise indicated). Transport at 25 °C was initiated by adding [^{35}S]sulfate (unless otherwise indicated) to substrate-loaded (exchange) or empty (uniport) proteoliposomes. Transport was terminated by adding 30 mM pyridoxal 5′-phosphate, which inhibits the activity of other MCs completely and rapidly [35,36]. In controls, the inhibitor was added at the beginning together with the radioactive substrate according to the "inhibitor-stop" method [30]. Finally, the external substrate was removed and the radioactivity in the proteoliposomes was measured. The experimental values were corrected by subtracting control values. In forward exchange kinetic experiments, the initial transport rates were calculated in mmol/min × g protein from the radioactivity incorporated into proteoliposomes in the initial linear range of substrate transport [37]. The kinetic constants K_m, V_{max} and K_i were determined from Lineweaver-Burk and Dixon plots. In some experiments the transport activity at 25 °C was determined by measuring the efflux of [^{35}S]sulfate in exchange for unlabeled substrates (backward exchange) [30]. In backward experiments, proteoliposomes containing 2 mM internal sulfate were loaded with 5 μM [^{35}S]sulfate by carrier-mediated exchange equilibrium [38]. The external radioactivity was removed by passing the proteoliposomes through Sephadex G-75 columns pre-equilibrated with 50 mM NaCl and 20 mM MES/MOPS pH 6.0. Efflux was started by adding unlabeled external substrate or NaCl and terminated by adding 30 mM pyridoxal 5′-phosphate. In backward exchange kinetic experiments (with 20 mM [^{35}S]sulfate inside and different external unlabeled substrate concentrations outside), the decrease in radioactivity was

fitted to a single exponential decay equation plus offset, and the initial rate was derived from this curve [39].

2.6. Other methods

Proteins were analyzed by SDS-PAGE and stained with Coomassie Blue dye. The identity of the bacterially expressed and purified UCP5L, UCP5S and UCP6 was assessed by matrix-assisted laser desorption/ionization-time-of-flight (MALDI-TOF) mass spectrometry of trypsin digests of the corresponding band excised from Coomassie-stained gels [40,41]. The amount of purified UCP5L, UCP5S and UCP6 proteins was estimated by laser densitometry of stained samples using carbonic anhydrase as protein standard [42,43]. The amount of protein incorporated into liposomes was measured as described [44] and was about 10% of protein added to the reconstitution mixture.

3. Results

3.1. Bioinformatic analysis of UCP5 and UCP6 sequences

When disregarding the 37-residue and 34-residue N-terminal extensions of UCP5L and UCP5S, respectively, the amino acids of UCP5 and UCP6 are 81% identical to each other, a value similar to that of known MC isoforms [45–47]. Moreover, the sequences of UCP5L, UCP5S and UCP6 contain the sequence characteristics of the MCF (Supplementary Fig. 1). The closest human relatives of UCP5 and UCP6 are: UCP4 (33% and 36% identity, respectively), UCP3 (31% and 35%), UCP2 (31% and 35%), the oxoglutarate carrier OGC (32% and 30%), UCP1 (28% and 31%) and the dicarboxylate carrier DIC (27% and 28%). These proteins cluster together in phylogenetic trees of human MCs [6] and all MCs in *H. sapiens*, *S. cerevisiae* and *A. thaliana* [48]. The present targeted phylogenetic analysis of the human UCPs and their closest relatives from species representative of various organisms coherently identified three well separated branches consisting of relatives of UCP4/UCP5/UCP6, UCP1/UCP2/UCP3 and DIC/OGC proteins (Fig. 1). On the first main branch UCP5 and UCP6 proteins form two close clusters, whereas UCP4 relatives form a different cluster. Thus, UCP5 and UCP6 sequences are phylogenetically closer to each other than to the UCP4 sequences or to any other UCP, DIC or OGC sequences.

3.2. Bacterial expression of UCP5L, UCP5S and UCP6

Reconstitution of recombinant proteins in liposomes is a commonly used method to identify and characterize the transport properties of carrier proteins encoded by different genomes [6]. Therefore, we expressed UCP5L, UCP5S and UCP6 in *E. coli* CO214(DE3) (Fig. 2, lanes 2, 5 and 8, respectively). UCP5SI was not expressed because the level of its transcript is very low and the existence of its translated product has not been confirmed [20]. After induction with isopropyl-β-D-thiogalactopyranoside, the proteins accumulated in the bacterial cytosol as inclusion bodies and were purified by centrifugation and washing (see Materials and methods). The apparent molecular masses of purified UCP5L, UCP5S and UCP6 (Fig. 2, lanes 3, 6 and 9) were approximately 33, 33 and 29 kDa, respectively, which are not very different from the calculated values of 36.2, 36.0 and 32.9 kDa for UCP5L, UCP5S and UCP6, respectively. The identity of the recombinant proteins was confirmed by MALDI-TOF mass spectrometry, and the yield of the purified proteins was about 60 mg per liter of culture. Notably, the proteins were not detected in bacteria harvested immediately before induction of expression (Fig. 2, lanes 1, 4 and 7) nor in cells harvested after induction but lacking the coding sequence in the expression vector (data not shown).

3.3. Functional characterization of UCP5L, UCP5S and UCP6

To explore the transport functions of UCP5L, UCP5S and UCP6, these proteins after their heterologous expression and purification were reconstituted into liposomes in active form using the sarkosyl refolding procedure (see Materials and methods). In a first set of experiments the reconstitution procedure was optimized by adjusting the parameters that influence the efficiency of active carrier incorporation into the liposomes. Optimal transport activity of [^{35}S]sulfate/sulfate exchange was obtained with 2.2 μg/ml protein for UCP5L and UCP5S and 4.4 μg/ml protein for UCP6, respectively, 12 mg/ml phospholipid concentration, a Triton-X114/phospholipid ratio of 0.9, 0.6 mg/ml cardiolipin and 14 passages through the same Amberlite column. Furthermore, the effect of pH on reconstitution of UCP5L, UCP5S and UCP6 was tested. Fig. 3 shows that the activities of UCP5L, UCP5S and UCP6 were greatly increased by decreasing the pH (inside and outside the proteoliposomes) from pH 8.0 to pH 6.0 and that UCP5L and UCP5S were more active than UCP6 at all pH values lower than 8.0. From hereon, only the results using UCP5L (named UCP5) will be reported given that virtually no difference in the results obtained using UCP5L and UCP5S was observed by changing the pH from 6.0 to 8.0 as well as in all the experiments described below.

In subsequent experiments the transport activities of UCP5 and UCP6 for various radioactive substrates were investigated in homo-exchange experiments. The uptake of externally-added radioactive substrate (1 mM) into proteoliposomes, containing the same non-radioactive internal substrate (20 mM) or no substrate (20 mM NaCl present), after one hour incubation shows the levels of antiport and uniport/background transport, respectively (Fig. 4). Both UCP5 and UCP6 catalyzed active [^{35}S]sulfate/sulfate, [^{33}P]Pi/Pi and [^{14}C]malate/malate homo-exchanges, whereas only UCP5 mediated low but significant homo-exchanges of citrate, aspartate and glutamate. In contrast, no significant UCP5- or UCP6-mediated transport was observed with glycine and 2-oxoglutarate (Fig. 4). The levels of the sulfate/sulfate, Pi/Pi and malate/malate homo-exchanges were higher with reconstituted UCP5 than reconstituted UCP6. Furthermore, with both proteins the sulfate/sulfate exchange was much higher than the Pi/Pi and malate/malate exchanges. Notably, control experiments showed that no [^{35}S]sulfate/sulfate exchange activity was detected if UCP5 and UCP6 had been boiled before incorporation into liposomes or if proteoliposomes were reconstituted with sarkosyl-solubilized material from bacterial cells lacking the expression vectors for these proteins or harvested immediately before induction of expression (data not shown). In addition, no [^{35}S]sulfate/sulfate exchange was observed using pure liposomes, e. g. without incorporated proteins. In all these experiments, pyridoxal 5′-phosphate was used to block the transport reactions mediated by UCP5 and UCP6 according to the inhibitor stop method (see Materials and methods).

The substrate specificities of UCP5 and UCP6 were further examined in hetero-exchange experiments by measuring the initial rate of [^{35}S]sulfate uptake into proteoliposomes preloaded with various potential substrates (Fig. 5). For both UCP5 and UCP6, the highest activities were observed with internally-loaded sulfate, thiosulfate, sulfite, phosphate, oxalate, malonate, maleate, L-malate, L-citramalate and D-citramalate. To a lesser extent, both proteins also exchanged [^{35}S]sulfate for succinate, L-tartrate, D-tartrate, L-aspartate and D-aspartate, and only UCP5 for internal glutamate, citrate, cis-aconitate, trans-aconitate and D,L-isocitrate. In contrast, the uptake of labeled sulfate was negligible with internal NaCl and no substrate (about 5–8%). This level of sulfate uptake was not significantly different from those observed with internal glutamate, citrate, cis-aconitate, trans-aconitate, and D,L-isocitrate for UCP6 (Fig. 5), as well as with internal fumarate, oxaloacetate, 2-oxoglutarate, ADP, pyruvate, lysine and alanine (Fig. 5) and AMP, ATP, GTP, CTP, glycine, serine, valine, asparagine, glutamine, ornithine, arginine, methionine, S-adenosylmethionine, carnitine, α-ketoisocaproate, choline, glutathione and phosphoenolpyruvate for both UCP5

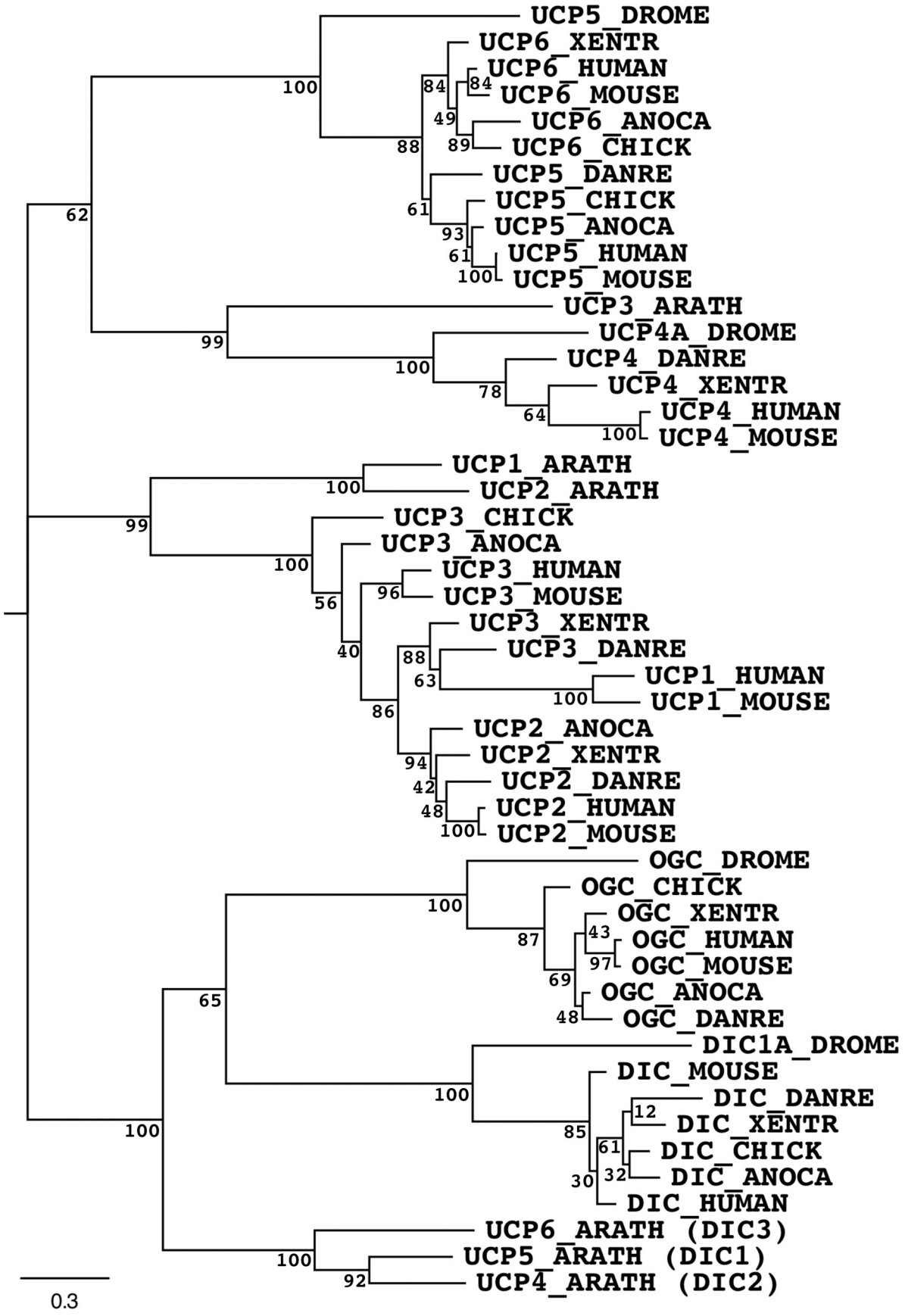

(caption on next page)

Fig. 1. Phylogenetic tree of uncoupling proteins (UCP), oxoglutarate carrier (OGC) and dicarboxylate carrier (DIC) from *H. sapiens* (HUMAN) and their closest relatives from *Drosophila melanogaster* (DROME), *Xenopus tropicalis* (XENTR), *Mus musculus* (MOUSE), *Anolis carolinensis* (ANOCA), *Gallus gallus* (CHICK), *Danio rerio* (DANRE) and *Arabidopsis thaliana* (ARATH). The tree was constructed with PhyML v3.1 from a multiple-sequence alignment with Muscle in Seaview4 and drawn in FigTree v1.4.2. Bootstrap values for 1000 replicates are reported on each node. The accession numbers of the sequences are: UCP5_DROME, NP_648501.1; UCP6_XENTR, NP_001165746.1; UCP6_HUMAN, NP_001010875.1; UCP6_MOUSE, NP_080508.1; UCP6_ANOCA, XP_003226660.1; UCP6_CHICK, XP_015132077.1; UCP5_DANRE, NP_956458.1; UCP5_CHICK, NP_001012901.1; UCP5_ANOCA, XP_003227137.1; UCP5_HUMAN, NP_001269124.1; UCP5_MOUSE, NP_001159922.1; UCP3_ARATH, NP_172866.1; UCP4A_DROME, NP_573246.1; UCP4_DANRE, NP_956635.1; UCP4_XENTR, NP_001011241.1; UCP4_HUMAN, NP_001190980.1; UCP4_MOUSE, NP_001344051.1; UCP1_ARATH, NP_190979.1; UCP2_ARATH, NP_568894.1; UCP3_CHICK, NP_989438.1; UCP3_ANOCA, XP_003229598.1; UCP3_HUMAN, NP_003347.1; UCP3_MOUSE, NP_033490.1; UCP3_XENTR, NP_001107354.1; UCP3_DANRE, NP_955817.1; UCP1_HUMAN, NP_068605.1; UCP1_MOUSE, NP_033489.1; UCP2_ANOCA, XP_008122231.1; UCP2_XENTR, NP_989179.1; UCP2_DANRE, NP_571251.1; UCP2_HUMAN, NP_003346.2; UCP2_MOUSE, NP_035801.3; OGC_DROME, NP_651703.1; OGC_CHICK, XP_025002025.1; OGC_XENTR, NP_001025683.1; OGC_HUMAN, NP_001158889.1; OGC_MOUSE, NP_077173.1; OGC_ANOCA, XP_008122732.1; OGC_DANRE, NP_001002099.1; DIC1A_DROME, NP_650279.1; DIC_MOUSE, NP_038798.2; DIC_DANRE, XP_002661286.1; DIC_XENTR, NP_001017018.1; DIC_CHICK, XP_015151037.1; DIC_ANOCA, XP_003217373.1; DIC_HUMAN, NP_001257817.1; UCP6_ARATH, NP_196509.1; UCP5_ARATH, NP_179836.1; and UCP4_ARATH, NP_194188.1.

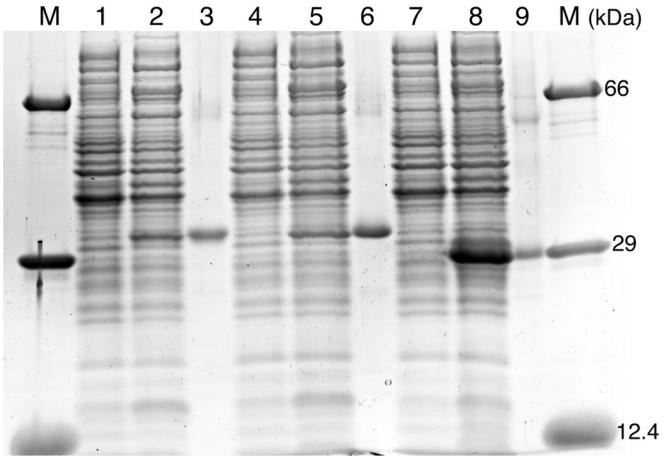

Fig. 2. Expression in *Escherichia coli* and purification of UCP5L, UCP5S and UCP6. Proteins were separated by SDS-PAGE and stained with Coomassie Blue. The following samples were loaded: markers (M), bovine serum albumin, carbonic anhydrase and cytochrome *c* of 66, 29 and 12.4 kDa, respectively; UCP5L (lanes 1–3); UCP5S (lanes 4–6); UCP6 (lanes 7–9). Lanes 1, 2, 4, 5, 7 and 8, samples of *E. coli* CO214(DE3) containing the expression vector with the coding sequence for UCP5L, UCP5S or UCP6 taken immediately before induction (lanes 1, 4 and 7) and 5 h later (lanes 2, 5 and 8). The same number of bacteria was analyzed in each sample. Lanes 3, 6 and 9: purified UCP5L (2 μg), UCP5S (3 μg) and UCP6 (2 μg) derived from bacteria shown in lanes 2, 5 and 8, respectively.

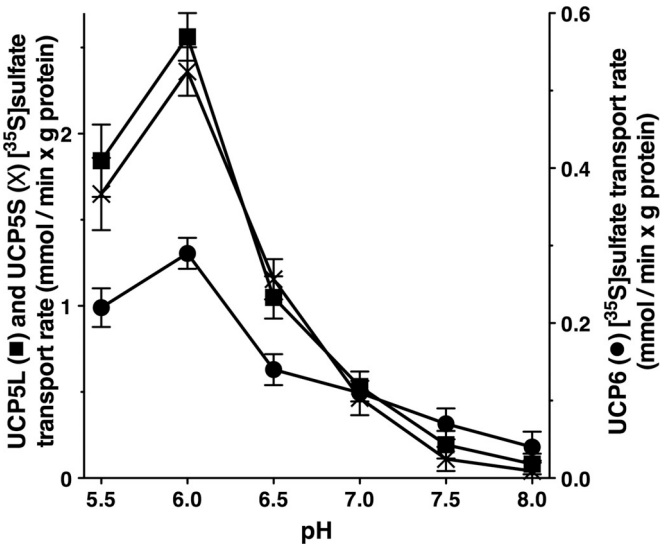

Fig. 3. The dependence of UCP5L-, UCP5S- and UCP6-mediated [^{35}S]sulfate/sulfate transport rates on the pH. The reconstitution mixture contained 20 mM MES/MOPS at the indicated pH values. After reconstitution of UCP5L, UCP5S and UCP6 into liposomes, 20 mM MES/MOPS with the same pH of the reconstitution mixture was used to equilibrate and elute the Sephadex G-75 columns. Transport was started by adding 1 mM [^{35}S]sulfate (in 20 mM MES/MOPS at the same pH as in the starting mixture) to the proteoliposomes and terminated after 30 s (UCP5L and UCP5S) or 1 min (UCP6). The values are means ± SEM of at least three independent experiments for each carrier.

and UCP6 (data not shown).

The effects of mitochondrial carrier inhibitors on the UCP5- and UCP6-mediated [^{35}S]sulfate/sulfate exchange reactions were also examined (Fig. 6). These transport activities were inhibited strongly by pyridoxal 5′-phosphate, bathophenanthroline and the organic mercurials mersalyl, p-chloromercuribenzoate and $HgCl_2$. They were also inhibited, to a lesser extent, by 4 mM butylmalonate, benzylmalonate and phenylsuccinate (mitochondrial DIC inhibitors) as well as by tannic acid and bromocresol purple (mitochondrial glutamate carrier inhibitors). Carboxyatractyloside and bongkrekic acid, which are specific and powerful inhibitors of the mitochondrial ADP/ATP carrier [49], exhibited a different behaviour: bongkrekic acid inhibited the activities of UCP5 and UCP6 partially, whereas carboxyatractyloside had little effect at a concentration (10 μM) that completely inhibits the ADP/ATP carrier. No or little inhibition was observed with N-ethylmaleimide and α-cyano-4-hydroxycinnamate, which are inhibitors of other characterized mitochondrial carriers.

3.4. Kinetic characteristics of recombinant UCP5 and UCP6

The time courses of 1 mM [^{35}S]sulfate uptake by liposomes reconstituted with UCP5 or UCP6, measured either as exchange (with 20 mM substrate inside the proteoliposomes, (●), (○), (■), (×), (□) and (Δ)) or as uniport (without internal substrate, (♦)), are shown in Fig. 7, A and B. Whereas the uniport uptake of [^{35}S]sulfate catalyzed by both UCP5 (A) and UCP6 (B) was very low, the [^{35}S]sulfate/sulfate exchange reactions mediated by these proteins were substantial. Furthermore, they followed first-order kinetics, isotopic equilibrium being approached exponentially. The rate constants and the initial rates of sulfate exchange deduced from the time-courses [30] were 0.044 and 0.018 min^{-1} and 2.34 and 0.27 mmol/min × g protein for UCP5 and UCP6, respectively. Fig. 7, A and B also shows that the amount of labeled sulfate taken up by UCP5- and UCP6-reconstituted liposomes in the presence of internal sulfate (●) or thiosulfate (○) was greater than that entering in the presence of internal Pi (■), malate (×) or sulfite (□). In contrast, the uptake of [^{35}S]sulfate in the presence of internal fumarate (Δ) was virtually indistinguishable from that taken up in the absence of any substrate inside the proteoliposomes. These results indicate that sulfate, thiosulfate, Pi, malate and sulfite are transported by UCP5 and UCP6 though with different efficiency, whereas fumarate is not.

The uniport mode of transport by UCP5 and UCP6 was further investigated by measuring the efflux of [^{35}S]sulfate from preloaded active proteoliposomes (Fig. 8, A and B), given that this experimental approach provides a more sensitive assay for unidirectional transport [30]. With both reconstituted carriers a substantial and rapid efflux

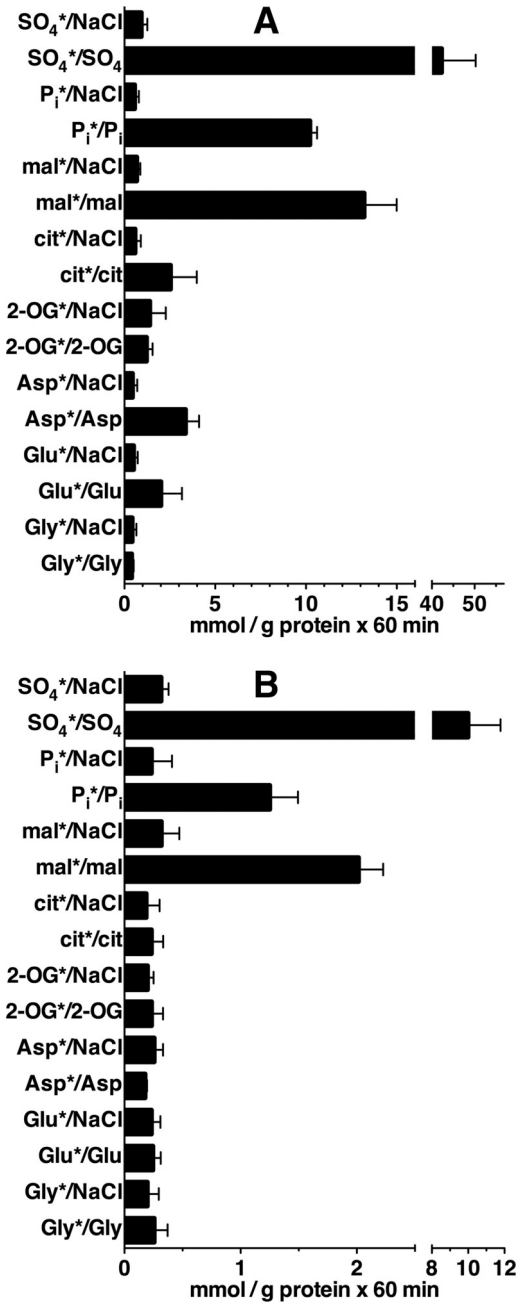

Fig. 4. UCP5- and UCP6-mediated homo-exchanges of various substrates. Proteoliposomes reconstituted with UCP5 (A) and UCP6 (B) were preloaded internally with the substrates or NaCl (concentration, 20 mM) as indicated in the figure. Transport was initiated by adding the radioactive substrate indicated by an asterisk (concentration, 1 mM) to proteoliposomes containing the same substrate or NaCl. The reaction was terminated after 60 min. The values are means ± SEM of at least three independent experiments. The differences between the amount of radioactive substrate taken up with internal NaCl and internal substrate were significant (Student's *t*-test, $p < 0.05$) for sulfate, phosphate and malate (for both UCP5 and UCP6) and aspartate (for UCP5). Abbreviations: mal, malate; cit, citrate; 2-OG, 2-oxoglutarate.

occurred upon addition of unlabelled sulfate (●) and thiosulfate (○) and, to a lower rate, upon addition of Pi (■), malate (×) and sulfite (□). By contrast, little and very low efflux of [^{35}S]sulfate was observed adding NaCl and no substrate (♦). Notably, upon addition of fumarate (Δ) the rates and extents of sulfate efflux were the same as those with NaCl, confirming that fumarate does not exchange with sulfate in liposomes reconstituted with UCP5 and UCP6. Furthermore, both efflux processes, i.e. those with and without external substrate, were prevented completely if the inhibitor pyridoxal 5′-phosphate was present from the beginning of the proteoliposome incubation ((◊) and (*)).

The kinetic constants of the recombinant purified UCP5 and UCP6 were determined by measuring the initial transport rate in the presence of various external [^{35}S]sulfate concentrations and a constant saturating internal concentration of 20 mM sulfate. The specific activities (Vmax) of UCP5 and UCP6 for the [^{35}S]sulfate/sulfate exchange were 4.7 ± 0.9 and 0.5 ± 0.1 mmol/min per g protein, respectively. The corresponding half-saturation constants (Km) for the uptake of [^{35}S]sulfate were 1.2 ± 0.1 mM (UCP5) and 0.7 ± 0.1 mM (UCP6) (Table 1). To determine the Km values for non-radioactive thiosulfate the backward exchange method [30,39] was applied. In these experiments the internal substrate pool of proteoliposomes contained 20 mM [^{35}S]sulfate, and the export of [^{35}S]sulfate was initiated by adding different concentrations of non-radioactive thiosulfate. From 4 experiments of this type, the Km values of UCP5 and UCP6 for thiosulfate were calculated to be 1.3 ± 0.1 and 0.8 ± 0.1 mM, respectively (Table 1). These values are similar to the inhibition constants (Ki) of thiosulfate, determined by measuring the [^{35}S]sulfate/sulfate exchange in the presence of different external thiosulfate concentrations (Table 1). The Km values for sulfate were also measured by the backward exchange method (in the presence of 20 mM internal [^{35}S]sulfate and different external sulfate concentrations) and found to be in agreement with those obtained from the forward exchange determinations (Table 1), demonstrating that the backward exchange technique is applicable to reconstituted UCP5 and UCP6.

Thiosulfate, sulfite, Pi and malate inhibited [^{35}S]sulfate/sulfate exchange catalyzed by both UCP5 and UCP6 competitively, because they increase the apparent Km without changing the Vmax of [^{35}S]sulfate uptake (data not shown). The inhibition constants (Ki) of these substrates for UCP5 and UCP6 are reported in Table 1.

3.5. Analysis of UCP5 and UCP6 homology models

Structural homology models of human UCP5 and UCP6, built on the 3D structure of the carboxyatractyloside-inhibited ADP/ATP carrier [50,51], show that positively charged residues in the three contact points of the proposed similarly-located substrate-binding site of MCs [52] are at positions compatible with binding sulfate (sulfite and thiosulfate, not shown) by salt bridges or H-bonds (Supplementary Fig. 2). Contact point II residues are thought to discriminate between the main substrate classes of MCs, i.e. for nucleotides (G-[IVLM]), carboxylates (R[QHNT]) and amino acids (R[DE]). UCP5 and UCP6 have RA in contact point II similarly to human, yeast and plant dicarboxylate carriers (R[GA]), which also transport sulfate, sulfite and thiosulfate [17,53,54].

4. Discussion

In this work heterologous expression, purification and reconstitution into liposomes (the EPRA method) [6] have been employed to investigate the hitherto unidentified transport functions of the close homologous proteins UCP5 and UCP6 from *H. sapiens*.

The transport properties and kinetic parameters of UCP5 and UCP6, as documented herein, are very similar, indicating that these two proteins are likely to share the same functions. They both transport sulfur oxyanions, phosphate and dicarboxylates and only UCP5 tricarboxylates to a very low extent. Furthermore, both proteins catalyze a fast counter-exchange of substrates and a very low unidirectional transport, respond similarly to the inhibitors tested and have similar half-saturation constants for sulfate and thiosulfate. However, they greatly differ for their specific activities (Vmax), UCP5 being much more active than UCP6, although both activities are similar or higher than those exhibited by most mitochondrial carriers characterized until now [6,48]. The substrate specificities of UCP5 and UCP6 are different from those of

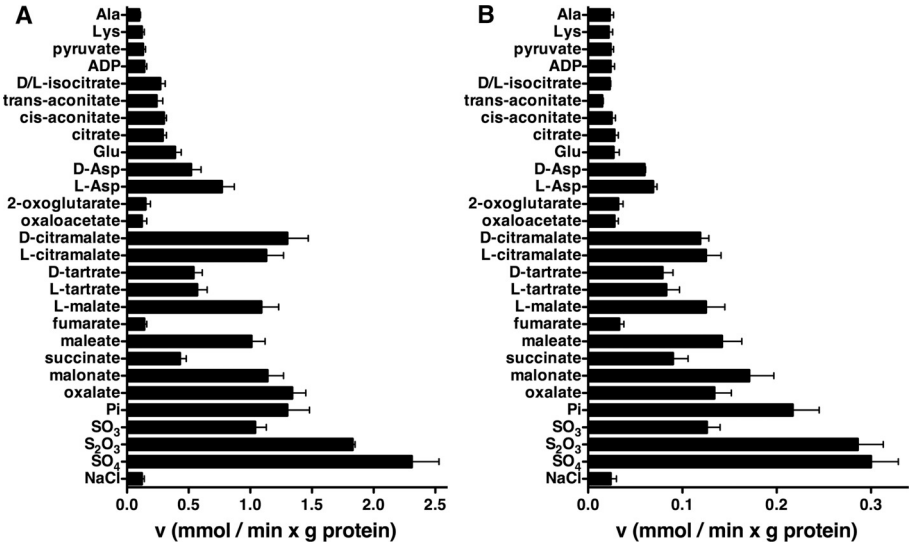

Fig. 5. Substrate specificity of UCP5 and UCP6. Proteoliposomes were preloaded internally with various substrates (concentration, 20 mM). Transport was started by adding 1 mM [^{35}S]sulfate and stopped after 30 s (UCP5) or 1 min (UCP6). The values are means ± SEM of at least three independent experiments. The differences between the activity of sulfate uptake with internal NaCl and the activities with internal metabolites were significant (Student's *t*-test, $p < 0.05$) except with internal fumarate, oxaloacetate, 2-oxoglutarate (2-OG), ADP, pyruvate, lysine and alanine (for both UCP5 and UCP6) and glutamate, citrate, isocitrate, cis-aconitate and trans-aconitate (for UCP6).

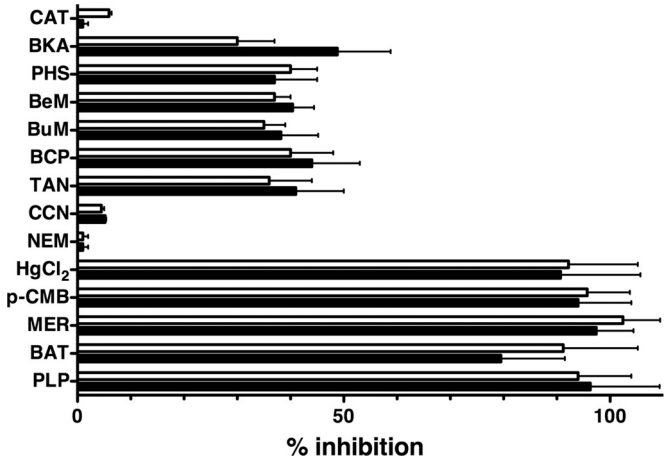

Fig. 6. Effect of mitochondrial carrier inhibitors on the rate of [^{35}S]sulfate/sulfate exchange mediated by UCP5 and UCP6. Liposomes were reconstituted with UCP5 and UCP6 and preloaded internally with 20 mM sulfate. Transport was initiated by adding 1 mM [^{35}S]sulfate and terminated after 30 s (UCP5) or 1 min (UCP6). Thiol reagents and α-cyanocinnamate were added 2 min before the labeled substrate; the other inhibitors were added together with [^{35}S]sulfate. The final concentrations of the inhibitors were: 10 μM ($HgCl_2$, mercuric chloride; BKA, bongkrekic acid; CAT, carboxyatractyloside), 0.1 mM (MER, mersalyl; p-CMB, p-chloromercuriobenzoate), 0.3 mM (BCP, bromocresol purple), 2 mM (PLP, pyridoxal 5′-phosphate; BAT, bathophenanthroline; NEM, N-ethylmaleimide; CCN, α-cyanocinnamate), 4 mM (BuM, butylmalonate; BeM, benzylmalonate; PHS, phenylsuccinate) and 0.1% (TAN, tannic acid). The data are means of % inhibition ± SEM of at least three independent experiments for UCP5 (black bars) and UCP6 (white bars).

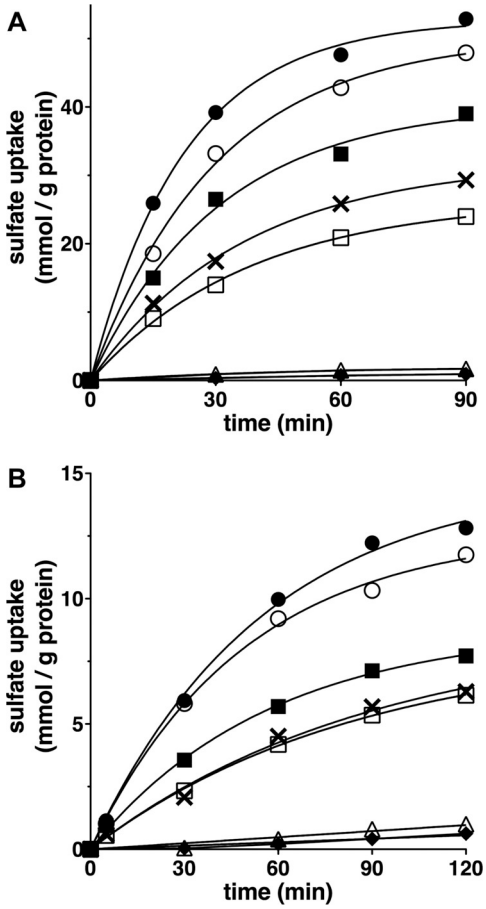

Fig. 7. Kinetics of [^{35}S]sulfate uptake by UCP5- and UCP6-reconstituted liposomes. Liposomes reconstituted with UCP5 (A) or UCP6 (B) were preloaded internally with 20 mM sulfate (●), thiosulfate (○), phosphate (■), malate (×), sulfite (□), fumarate (Δ) or 20 mM NaCl and no substrate (♦). Transport was initiated by adding 1 mM [^{35}S]sulfate and terminated at the indicated times. Similar results were obtained in at least three independent experiments.

any other mitochondrial carrier identified until now in yeast, mammals and plants [6,48] including their closest relatives UCPs, OGC and DIC. The functionally identified UCPs differ from UCP5 and UCP6 because hUCP1 is a H^+ transporter [7,8], hUCP2 transports aspartate as efficiently as malate [18], AtUCP1-2 transport aspartate, glutamate and dicarboxylates equally well [19] and AtUCP4-6 are three isoforms of the genuine dicarboxylate carrier in yeast, mammals and plants [17,53–55]. Several protein sequences available in databases are likely to be orthologs of UCP5 and UCP6. These sequences include: UCP5 and UCP6 from *Mus musculus* (98% and 92% sequence identity with human UCP5 and UCP6, respectively), UCP5 and UCP6 from *Anolis carolinensis* (81% and 79% identity with their human counterparts, respectively), UCP5 and UCP6 from *Gallus gallus* (78% and 87% identity with their human counterparts, respectively), UCP5 from *Danio rerio* (70% identity with hUCP5 and 79% with hUCP6), UCP6 from *Xenopus tropicalis* (72% identity with hUCP5 and 89% hUCP6) and UCP5 from *Drosophila melanogaster* (48% identity with hUCP5 and 56% hUCP6). To our

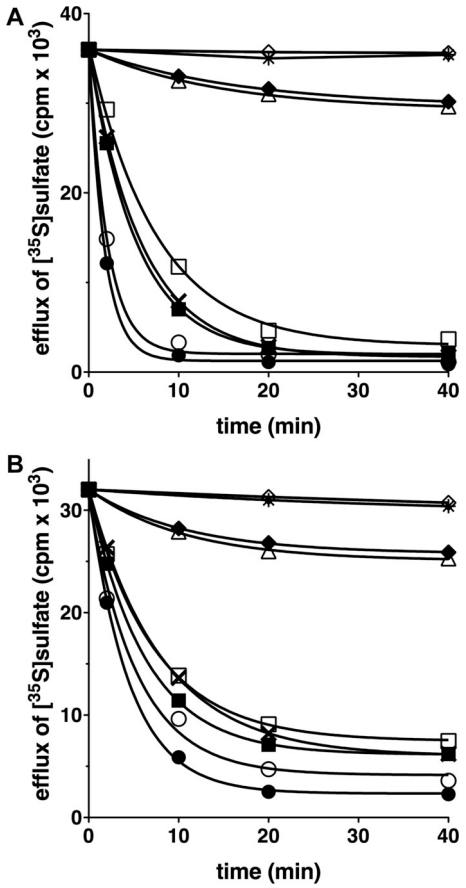

Fig. 8. Kinetics of [^{35}S]sulfate efflux from UCP5- and UCP6-reconstituted liposomes. Liposomes reconstituted with UCP5 (A) or UCP6 (B) and containing 2 mM sulfate internally were preloaded with [^{35}S]sulfate by carrier-mediated exchange equilibrium; then the external substrate was removed by Sephadex G-75. Efflux of [^{35}S]sulfate was started by adding 10 mM sulfate (●), thiosulfate (○), phosphate (■), malate (×), sulfite (□), fumarate (Δ),10 mM NaCl and no substrate (◆), 10 mM sulfate together with 30 mM pyridoxal 5′-phosphate (◊) or 30 mM pyridoxal 5′-phosphate and no substrate (*). The transport was terminated at the indicated times. Similar results were obtained in at least three independent experiments.

Table 1
Km and Ki of recombinant UCP5 and UCP6 for sulfate and other substrates. To determine the Km values in forward exchange (f) and Ki values the proteoliposomes were loaded with 20 mM sulfate and transport was started by adding varying concentrations of external [^{35}S]sulfate (with or without increasing concentrations of the indicated competing substrates for Ki). To determine the Km values in backward exchange (b) the proteoliposomes were loaded with 20 mM [^{35}S]sulfate and transport was started by adding increasing concentrations of external non-radioactive sulfate or thiosulfate. The reaction time was 30 s for UCP5 and 1 min for UCP6. Other experimental conditions as in Materials and Methods. The values are means ± SEM of at least three independent experiments in duplicate.

Substrate	UCP5		UCP6	
	Km (mM)	Ki (mM)	Km (mM)	Ki (mM)
Sulfate	1.2 ± 0.1 (f)		0.7 ± 0.1 (f)	
Sulfate	1.2 ± 0.2 (b)		0.8 ± 0.1 (b)	
Thiosulfate	1.3 ± 0.1 (b)	1.3 ± 0.1	0.8 ± 0.1 (b)	0.8 ± 0.1
Phosphate		1.6 ± 0.2		1.7 ± 0.2
Malate		2.1 ± 0.2		1.9 ± 0.2
Sulfite		2.4 ± 0.3		1.9 ± 0.2

b, backward exchange; f, forward exchange.

knowledge, none of these proteins have been characterized biochemically. Interestingly, orthologs of human UCP5 and UCP6 are found in mammals, reptiles and birds, whereas fish, amphibians and insects have single orthologs of UCP5/6 (Fig. 1) and plants no one.

Two additional remarks regarding the transport properties of UCP5 and UCP6 should be made. Firstly, the close biochemical similarities between UCP5/6 are understandable given the commonality of their gene structures; both genes (*SLC25A14* and *SLC25A30*) share an identical exon/intron structure (which is different from those of the other UCPs). We, therefore, assume that UCP5/6 derive from a common molecular ancestor accounting for the similarities in their biochemical properties. Subsequently, once gene duplication took place, independent evolution allowed the development of individual properties such as the differences in expression regulation, specific activity and substrate preference. Secondly, our transport measurements on UCP5 and UCP6, in agreement with previous data on AtUCP4-6 [17], hUCP2 [18] and AtUCP1-2 [19], demonstrate that most MCs previously designated “uncoupling proteins” transport metabolites. Therefore, the name UCP for these proteins, with the exception of mammalian UCP1, does not seem to be appropriate.

In previous publications both UCP5 and UCP6 have been implicated in the regulation of reactive oxygen species (ROS). It has been shown that UCP5 overexpression lowers the accumulation of ROS in neuronal GT1-1 and SH-SY5Y neuroblastoma cells [21,22], whereas UCP5 silencing increases ROS production in osteosarcoma U2OS cells [56]. A reciprocal relationship between ROS and UCP5 has also been observed in brain; induction of ROS generation causes marked up-regulation of UCP5, whereas hypoxia reduces UCP5 expression in neuroblastoma SK-N-SH and SH-SY5Y cells, in rat brain cortex, as well as in colon cancer progression HT-29, SW-620 and HT-29(Glu-R) cells [57–59]. Furthermore, it has been speculated that UCP5 plays a role in transient cerebral ischemia [58,60]. Regarding UCP6, its expression is increased upon fasting and during the regenerative phase of glycerol-induced renal failure, conditions that are associated with transiently increased expression of superoxide-generating enzymes, mitochondrial metabolism and antioxidant defences [16]. Thus, it seems that UCP5 and UCP6 have similar roles in ROS reduction.

Given the preference of UCP5/6 for sulfate and thiosulfate as transported substrates, their ability to transport sulfite rather efficiently as well as their reported association with the regulation of ROS, we propose that a main physiological role of UCP5/6 is probably to modulate the concentration of the important gaseous signaling molecule H_2S by catalyzing the efflux of the H_2S degradation products sulfite and thiosulfate from mitochondria in exchange with sulfate, phosphate or a dicarboxylate (malate) (Fig. 9). H_2S is synthesized by four pathways; the enzymes of two of them are cytosolic, whereas the last enzyme of the remaining two pathways is localized in mitochondria [61,62]. The degradation of H_2S takes place in the mitochondrial matrix by the action of SQR (sulfide:quinone oxidoreductase) and SDO (sulfur dioxygenase) to produce sulfite [63], and SQR and TST (thiosulfate sulfurtransferase or rhodanase) to produce thiosulfate from sulfite [61,62] (Fig. 9). Sulfate is also produced from sulfite by sulfite oxidase (SO), which is localized in the mitochondrial intermembrane space. The enzymes of H_2S synthesis and all the H_2S-degrading enzymes are present in several tissues including brain and kidney [64–67]. H_2S, whose cellular concentration is determined by its synthesis and degradation rates, has several relevant physiological functions, among which a major one is to protect cells from ROS damage [62,68,69]. Importantly, H_2S displays its antioxidant effect only at low concentration, whereas at higher concentrations it may even act as an oxidant [68,69].

The proposal that mitochondrial export of thiosulfate and sulfite is a primary function of UCP5 and UCP6, at least in brain and kidney cortex, is consistent with the observation that H_2S has high turnover rates in these tissues [65] (due to the presence of multiple enzymes of H_2S biosynthesis and clearance) and with the prevalent expression of UCP5 and UCP6 in the mitochondria of these organs. Furthermore, in hypoxic

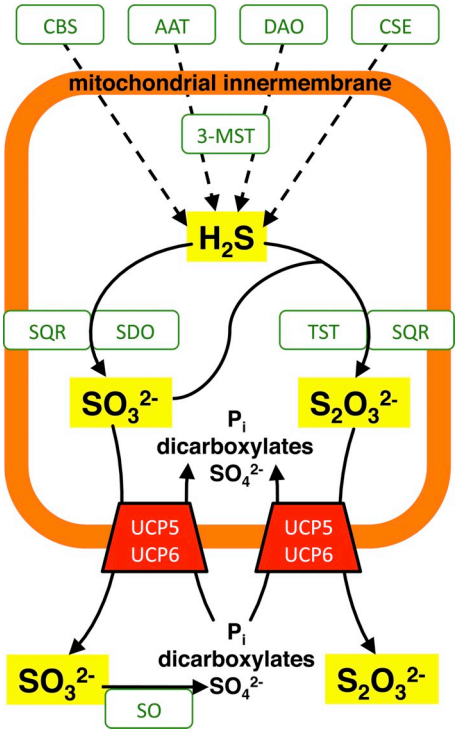

Fig. 9. Proposed metabolic roles of UCP5 and UCP6 in the mitochondrial export of the H_2S degradation products sulfite and thiosulfate in exchange with phosphate, a dicarboxylate or sulfate. The enzymes involved in H_2S synthesis and oxidation are abbreviated in green: 3-MST, 3-mercaptopyruvate sulfurtransferase; AAT, aspartate aminotransferase; CBS, cystathionine β-synthase; CSE, cystathionine γ-lyase; DAO, D-aminoacid oxidase; SDO, sulfur dioxygenase; SO, sulfite oxidase; SQR, sulfide:quinone oxidoreductase; TST, thiosulfate sulfurtransferase or rhodanase.

conditions H_2S production in brain is induced to maintain adequate supply of oxygen by cerebral vasodilation [70]. Hypoxic conditions also occur in parts of kidney, even under physiological conditions, and H_2S synthesis is induced [62,68]. It has been shown that the concentration of H_2S in the renal cortex is lower than in the renal medulla because mitochondrial H_2S oxidation is fast [62]. It is very likely that, under all these conditions, brain and renal cortex require the activity of UCP5 and UCP6 to contribute to decrease H_2S concentration to keep ROS level low and not to have cytochrome c oxidase inhibited.

Transparency document

The Transparency document associated with this article can be found, in online version.

Acknowledgements

This work was supported by the Italian Ministero dell'Istruzione, dell'Università e della Ricerca, MIUR (PRIN project 20158EB2CM_002), the Center of Excellence on Comparative Genomics and the CNR Institute of Biomembranes, Bioenergetics and Molecular Biotechnologies (IBIOM). We also acknowledge the expert technical assistance of Mr. Riccardo Merafina.

Appendix A. Supplementary data

Supplementary data to this article can be found online at https://doi.org/10.1016/j.bbabio.2019.07.010.

References

[1] R. Krämer, F. Palmieri, Metabolite carriers in mitochondria, in: L. Ernster (Ed.), Mol. Mech. Bioenerg, Elsevier, Amsterdam, 1992, pp. 359–384, , https://doi.org/10.1016/S0167-7306(08)60184-2.
[2] F. Palmieri, The mitochondrial transporter family SLC25: identification, properties and physiopathology, Mol. Asp. Med. 34 (2013) 465–484, https://doi.org/10.1016/j.mam.2012.05.005.
[3] F. Palmieri, Mitochondrial transporters of the SLC25 family and associated diseases: a review, J. Inherit. Metab. Dis. 37 (2014) 565–575, https://doi.org/10.1007/s10545-014-9708-5.
[4] F. Palmieri, Mitochondrial carrier proteins, FEBS Lett. 346 (1994) 48–54, https://doi.org/10.1016/0014-5793(94)00329-7.
[5] F. Palmieri, C.L. Pierri, Mitochondrial metabolite transport, Essays Biochem. 47 (2010) 37–52, https://doi.org/10.1042/bse0470037.
[6] F. Palmieri, M. Monné, Discoveries, metabolic roles and diseases of mitochondrial carriers: a review, Biochim. Biophys. Acta 1863 (2016) 2362–2378, https://doi.org/10.1016/j.bbamcr.2016.03.007.
[7] M. Klingenberg, E. Winkler, The reconstituted isolated uncoupling protein is a membrane potential driven H+ translocator, EMBO J. 4 (1985) 3087–3092, https://doi.org/10.1002/j.1460-2075.1985.tb04049.x.
[8] D.G. Nicholls, The physiological regulation of uncoupling proteins, Biochim. Biophys. Acta 1757 (2006) 459–466, https://doi.org/10.1016/j.bbabio.2006.02.005.
[9] D. Sanchis, C. Fleury, N. Chomiki, M. Goubern, Q. Huang, M. Neverova, F. Grégoire, J. Easlick, S. Raimbault, C. Lévi-Meyrueis, B. Miroux, S. Collins, M. Seldin, D. Richard, C. Warden, F. Bouillaud, D. Ricquier, BMCP1, a novel mitochondrial carrier with high expression in the central nervous system of humans and rodents, and respiration uncoupling activity in recombinant yeast, J. Biol. Chem. 273 (1998) 34611–34615, https://doi.org/10.1074/jbc.273.51.34611.
[10] M. Jaburek, M. Varecha, R.E. Gimeno, M. Dembski, P. Jezek, M. Zhang, P. Burn, L.A. Tartaglia, K.D. Garlid, Transport function and regulation of mitochondrial uncoupling proteins 2 and 3, J. Biol. Chem. 274 (1999) 26003–26007, https://doi.org/10.1074/jbc.274.37.26003.
[11] B.D. Fink, Y.-S. Hong, M.M. Mathahs, T.D. Scholz, J.S. Dillon, W.I. Sivitz, UCP2-dependent proton leak in isolated mammalian mitochondria, J. Biol. Chem. 277 (2002) 3918–3925, https://doi.org/10.1074/jbc.M107955200.
[12] M. Zackova, E. Skobisová, E. Urbánková, P. Jezek, Activating omega-6 polyunsaturated fatty acids and inhibitory purine nucleotides are high affinity ligands for novel mitochondrial uncoupling proteins UCP2 and UCP3, J. Biol. Chem. 278 (2003) 20761–20769, https://doi.org/10.1074/jbc.M212850200.
[13] M. Jaburek, K.D. Garlid, Reconstitution of recombinant uncoupling proteins: UCP1, -2, and -3 have similar affinities for ATP and are unaffected by coenzyme Q10, J. Biol. Chem. 278 (2003) 25825–25831, https://doi.org/10.1074/jbc.M302126200.
[14] T. Hoang, M.D. Smith, M. Jelokhani-Niaraki, Toward understanding the mechanism of ion transport activity of neuronal uncoupling proteins UCP2, UCP4, and UCP5, Biochemistry. 51 (2012) 4004–4014, https://doi.org/10.1021/bi3003378.
[15] H. Perreten Lambert, M. Zenger, G. Azarias, J.-Y. Chatton, P.J. Magistretti, S. Lengacher, Control of mitochondrial pH by uncoupling protein 4 in astrocytes promotes neuronal survival, J. Biol. Chem. 289 (2014) 31014–31028, https://doi.org/10.1074/jbc.M114.570879.
[16] A. Haguenauer, S. Raimbault, S. Masscheleyn, M. del M. Gonzalez-Barroso, F. Criscuolo, J. Plamondon, B. Miroux, D. Ricquier, D. Richard, F. Bouillaud, C. Pecqueur, A new renal mitochondrial carrier, KMCP1, is up-regulated during tubular cell regeneration and induction of antioxidant enzymes, J. Biol. Chem. 280 (2005) 22036–22043, https://doi.org/10.1074/jbc.M412136200.
[17] L. Palmieri, N. Picault, R. Arrigoni, E. Besin, F. Palmieri, M. Hodges, Molecular identification of three Arabidopsis thaliana mitochondrial dicarboxylate carrier isoforms: organ distribution, bacterial expression, reconstitution into liposomes and functional characterization, Biochem. J. 410 (2008) 621–629, https://doi.org/10.1042/BJ20070867.
[18] A. Vozza, G. Parisi, F. De Leonardis, F.M. Lasorsa, A. Castegna, D. Amorese, R. Marmo, V.M. Calcagnile, L. Palmieri, D. Ricquier, E. Paradies, P. Scarcia, F. Palmieri, F. Bouillaud, G. Fiermonte, UCP2 transports C4 metabolites out of mitochondria, regulating glucose and glutamine oxidation, Proc. Natl. Acad. Sci. U. S. A. 111 (2014) 960–965, https://doi.org/10.1073/pnas.1317400111.
[19] M. Monné, L. Daddabbo, D. Gagneul, T. Obata, B. Hielscher, L. Palmieri, D.V. Miniero, A.R. Fernie, A.P.M. Weber, F. Palmieri, Uncoupling proteins 1 and 2 (UCP1 and UCP2) from Arabidopsis thaliana are mitochondrial transporters of aspartate, glutamate, and dicarboxylates, J. Biol. Chem. 293 (2018) 4213–4227, https://doi.org/10.1074/jbc.RA117.000771.
[20] X.X. Yu, W. Mao, A. Zhong, P. Schow, J. Brush, S.W. Sherwood, S.H. Adams, G. Pan, Characterization of novel UCP5/BMCP1 isoforms and differential regulation of UCP4 and UCP5 expression through dietary or temperature manipulation, FASEB J. 14 (2000) 1611–1618, https://doi.org/10.1096/fj.99-0834com.
[21] J.S. Kim-Han, S.A. Reichert, K.L. Quick, L.L. Dugan, BMCP1: a mitochondrial uncoupling protein in neurons which regulates mitochondrial function and oxidant production, J. Neurochem. 79 (2001) 658–668, https://doi.org/10.1046/j.1471-4159.2001.00604.x.
[22] K.H.-H. Kwok, P.W.-L. Ho, A.C.-Y. Chu, J.W.-M. Ho, H.-F. Liu, D.C.-W. Yiu, K.-H. Chan, M.H.-W. Kung, D.B. Ramsden, S.-L. Ho, Mitochondrial UCP5 is neuroprotective by preserving mitochondrial membrane potential, ATP levels, and reducing oxidative stress in MPP+ and dopamine toxicity, Free Radic. Biol. Med. 49 (2010) 1023–1035, https://doi.org/10.1016/j.freeradbiomed.2010.06.017.
[23] G. Fiermonte, J.E. Walker, F. Palmieri, Abundant bacterial expression and reconstitution of an intrinsic membrane-transport protein from bovine mitochondria, Biochem. J. 294 (1993) 293–299, https://doi.org/10.1042/bj2940293.
[24] C.M.T. Marobbio, G. Giannuzzi, E. Paradies, C.L. Pierri, F. Palmieri, α-Isopropylmalate, a leucine biosynthesis intermediate in yeast, is transported by the mitochondrial oxalacetate carrier, J. Biol. Chem. 283 (2008) 28445–28553, https://

doi.org/10.1074/jbc.M804637200.
[25] G. Agrimi, A. Russo, P. Scarcia, F. Palmieri, The human gene SLC25A17 encodes a peroxisomal transporter of coenzyme A, FAD and NAD+, Biochem. J. 443 (2012) 241–247, https://doi.org/10.1042/BJ20111420.
[26] G. Agrimi, A. Russo, C.L. Pierri, F. Palmieri, The peroxisomal NAD+ carrier of Arabidopsis thaliana transports coenzyme A and its derivatives, J. Bioenerg. Biomembr. 44 (2012) 333–340, https://doi.org/10.1007/s10863-012-9445-0.
[27] M.A. Di Noia, S. Todisco, A. Cirigliano, T. Rinaldi, G. Agrimi, V. Iacobazzi, F. Palmieri, The human SLC25A33 and SLC25A36 genes of solute carrier family 25 encode two mitochondrial pyrimidine nucleotide transporters, J. Biol. Chem. 289 (2014) 33137–33148, https://doi.org/10.1074/jbc.M114.610808.
[28] S. Cavero, A. Vozza, A. Del Arco, L. Palmieri, A. Villa, E. Blanco, M.J. Runswick, J.E. Walker, S. Cerdán, F. Palmieri, J. Satrústegui, Identification and metabolic role of the mitochondrial aspartate-glutamate transporter in Saccharomyces cerevisiae, Mol. Microbiol. 50 (2003) 1257–1269, https://doi.org/10.1046/j.1365-2958.2003.03742.x.
[29] L. Palmieri, R. Arrigoni, E. Blanco, F. Carrari, M.I. Zanor, C. Studart-Guimaraes, A.R. Fernie, F. Palmieri, Molecular identification of an Arabidopsis S-adenosylmethionine transporter. Analysis of organ distribution, bacterial expression, reconstitution into liposomes, and functional characterization, Plant Physiol. 142 (2006) 855–865, https://doi.org/10.1104/pp.106.086975.
[30] F. Palmieri, C. Indiveri, F. Bisaccia, V. Iacobazzi, Mitochondrial metabolite carrier proteins: purification, reconstitution, and transport studies, Methods Enzymol. 260 (1995) 349–369, https://doi.org/10.1016/0076-6879(95)60150-3.
[31] F. Bisaccia, F. Palmieri, Specific elution from hydroxylapatite of the mitochondrial phosphate carrier by cardiolipin, Biochim. Biophys. Acta 766 (1984) 386–394, https://doi.org/10.1016/0005-2728(84)90254-8.
[32] B. Kadenbach, P. Mende, H.V. Kolbe, I. Stipani, F. Palmieri, The mitochondrial phosphate carrier has an essential requirement for cardiolipin, FEBS Lett. 139 (1982) 109–112, https://doi.org/10.1016/0014-5793(82)80498-5.
[33] C. Indiveri, A. Tonazzi, F. Palmieri, Characterization of the unidirectional transport of carnitine catalyzed by the reconstituted carnitine carrier from rat liver mitochondria, Biochim. Biophys. Acta 1069 (1991) 110–116, https://doi.org/10.1016/0005-2736(91)90110-t.
[34] C. Indiveri, A. Tonazzi, G. Prezioso, F. Palmieri, Kinetic characterization of the reconstituted carnitine carrier from rat liver mitochondria, Biochim. Biophys. Acta 1065 (1991) 231–238, https://doi.org/10.1016/0005-2736(91)90235-z.
[35] G. Fiermonte, V. Dolce, F. Palmieri, Expression in Escherichia coli, functional characterization, and tissue distribution of isoforms A and B of the phosphate carrier from bovine mitochondria, J. Biol. Chem. 273 (1998) 22782–22787, https://doi.org/10.1074/jbc.273.35.2278.
[36] A. Castegna, P. Scarcia, G. Agrimi, L. Palmieri, H. Rottensteiner, I. Spera, L. Germinario, F. Palmieri, Identification and functional characterization of a novel mitochondrial carrier for citrate and oxoglutarate in S. cerevisiae, J. Biol. Chem. 285 (2010) 17359–17370, https://doi.org/10.1074/jbc.M109.097188.
[37] L. Palmieri, F.M. Lasorsa, V. Iacobazzi, M.J. Runswick, F. Palmieri, J.E. Walker, Identification of the mitochondrial carnitine carrier in Saccharomyces cerevisiae, FEBS Lett. 462 (1999) 472–476, https://doi.org/10.1016/S0014-5793(99)01555-0.
[38] C.M.T. Marobbio, M.A. Di Noia, F. Palmieri, Identification of a mitochondrial transporter for pyrimidine nucleotides in Saccharomyces cerevisiae: bacterial expression, reconstitution and functional characterization, Biochem. J. 393 (2006) 441–446, https://doi.org/10.1042/BJ20051284.
[39] L. Palmieri, F.M. Lasorsa, A. De Palma, F. Palmieri, M.J. Runswick, J.E. Walker, Identification of the yeast ACR1 gene product as a succinate-fumarate transporter essential for growth on ethanol or acetate, FEBS Lett. 417 (1997) 114–118, https://doi.org/10.1016/S0014-5793(97)01269-6.
[40] L. Palmieri, G. Agrimi, M.J. Runswick, I.M. Fearnley, F. Palmieri, J.E. Walker, Identification in Saccharomyces cerevisiae of two isoforms of a novel mitochondrial transporter for 2-oxoadipate and 2-oxoglutarate, J. Biol. Chem. 276 (2001) 1916–1922, https://doi.org/10.1074/jbc.M004332200.
[41] M.E. Hoyos, L. Palmieri, T. Wertin, R. Arrigoni, J.C. Polacco, F. Palmieri, Identification of a mitochondrial transporter for basic amino acids in Arabidopsis thaliana by functional reconstitution into liposomes and complementation in yeast, Plant J. 33 (2003) 1027–1035, https://doi.org/10.1046/j.1365-313X.2003.01685.x.
[42] C. Indiveri, V. Iacobazzi, N. Giangregorio, F. Palmieri, Bacterial overexpression, purification, and reconstitution of the carnitine/acylcarnitine carrier from rat liver mitochondria, Biochem. Biophys. Res. Commun. 249 (1998) 589–594, https://doi.org/10.1006/bbrc.1998.9197.
[43] M. Monné, D.V. Miniero, T. Obata, L. Daddabbo, L. Palmieri, A. Vozza, M.C. Nicolardi, A.R. Fernie, F. Palmieri, Functional characterization and organ distribution of three mitochondrial ATP-Mg/Pi carriers in Arabidopsis thaliana, Biochim. Biophys. Acta 1847 (2015) 1220–1230, https://doi.org/10.1016/j.bbabio.2015.06.015.
[44] V. Porcelli, G. Fiermonte, A. Longo, F. Palmieri, The human gene SLC25A29, of solute carrier family 25, encodes a mitochondrial transporter of basic amino acids, J. Biol. Chem. 289 (2014) 13374–13384, https://doi.org/10.1074/jbc.M114.547448.
[45] G. Fiermonte, L. Palmieri, S. Todisco, G. Agrimi, F. Palmieri, J.E. Walker, Identification of the mitochondrial glutamate transporter. Bacterial expression, reconstitution, functional characterization, and tissue distribution of two human isoforms, J. Biol. Chem. 277 (2002) 19289–19294, https://doi.org/10.1074/jbc.M201572200.
[46] G. Fiermonte, V. Dolce, L. David, F.M. Santorelli, C. Dionisi-Vici, F. Palmieri, J.E. Walker, The mitochondrial ornithine transporter. Bacterial expression, reconstitution, functional characterization, and tissue distribution of two human isoforms, J. Biol. Chem. 278 (2003) 32778–32783, https://doi.org/10.1074/jbc.M302317200.
[47] F. Palmieri, B. Rieder, A. Ventrella, E. Blanco, P.T. Do, A. Nunes-Nesi, A.U. Trauth, G. Fiermonte, J. Tjaden, G. Agrimi, S. Kirchberger, E. Paradies, A.R. Fernie, H.E. Neuhaus, Molecular identification and functional characterization of Arabidopsis thaliana mitochondrial and chloroplastic NAD+ carrier proteins, J. Biol. Chem. 284 (2009) 31249–31259, https://doi.org/10.1074/jbc.M109.041830.
[48] F. Palmieri, C.L. Pierri, A. De Grassi, A. Nunes-Nesi, A.R. Fernie, Evolution, structure and function of mitochondrial carriers: a review with new insights, Plant J. 66 (2011) 161–181, https://doi.org/10.1111/j.1365-313X.2011.04516.x.
[49] M. Klingenberg, The ADP and ATP transport in mitochondria and its carrier, Biochim. Biophys. Acta 1778 (2008) 1978–2021, https://doi.org/10.1016/j.bbamem.2008.04.011.
[50] E. Pebay-Peyroula, C. Dahout-Gonzalez, R. Kahn, V. Trézéguet, G.J.-M. Lauquin, G. Brandolin, Structure of mitochondrial ADP/ATP carrier in complex with carboxyatractyloside, Nature. 426 (2003) 39–44, https://doi.org/10.1038/nature02056.
[51] J.J. Ruprecht, A.M. Hellawell, M. Harding, P.G. Crichton, A.J. McCoy, E.R.S. Kunji, Structures of yeast mitochondrial ADP/ATP carriers support a domain-based alternating-access transport mechanism, Proc. Natl. Acad. Sci. U. S. A. 111 (2014) E426–E434, https://doi.org/10.1073/pnas.1320692111.
[52] A.J. Robinson, E.R.S. Kunji, Mitochondrial carriers in the cytoplasmic state have a common substrate binding site, Proc. Natl. Acad. Sci. U. S. A. 103 (2006) 2617–2622, https://doi.org/10.1073/pnas.0509994103.
[53] L. Palmieri, F. Palmieri, M.J. Runswick, J.E. Walker, Identification by bacterial expression and functional reconstitution of the yeast genomic sequence encoding the mitochondrial dicarboxylate carrier protein, FEBS Lett. 399 (1996) 299–302, https://doi.org/10.1016/S0014-5793(96)01350-6.
[54] G. Fiermonte, L. Palmieri, V. Dolce, F.M. Lasorsa, F. Palmieri, M.J. Runswick, J.E. Walker, The sequence, bacterial expression, and functional reconstitution of the rat mitochondrial dicarboxylate transporter cloned via distant homologs in yeast and Caenorhabditis elegans, J. Biol. Chem. 273 (1998) 24754–24759, https://doi.org/10.1074/jbc.273.38.24754.
[55] G. Fiermonte, V. Dolce, R. Arrigoni, M.J. Runswick, J.E. Walker, F. Palmieri, Organization and sequence of the gene for the human mitochondrial dicarboxylate carrier: evolution of the carrier family, Biochem. J. 344 (Pt 3) (1999) 953–960, https://doi.org/10.1042/bj3440953.
[56] W.T. Senapedis, C.J. Kennedy, P.M. Boyle, P.A. Silver, Whole genome siRNA cell-based screen links mitochondria to Akt signaling network through uncoupling of electron transport chain, Mol. Biol. Cell 22 (2011) 1791–1805, https://doi.org/10.1091/mbc.E10-10-0854.
[57] P.W.-L. Ho, D.Y.-L. Chan, K.H.-H. Kwok, A.C.-Y. Chu, J.W.-M. Ho, M.H.-W. Kung, D.B. Ramsden, S.-L. Ho, Methyl-4-phenylpyridinium ion modulates expression of mitochondrial uncoupling proteins 2, 4, and 5 in catecholaminergic (SK-N-SH) cells, J. Neurosci. Res. 81 (2005) 261–268, https://doi.org/10.1002/jnr.20569.
[58] P. Pichiule, J.C. Chavez, J.C. LaManna, Oxygen and oxidative stress modulate the expression of uncoupling protein-5 in vitro and in vivo, Adv. Exp. Med. Biol. 540 (2003) 103–107, https://doi.org/10.1007/978-1-4757-6125-2_15.
[59] F.M. Santandreu, A. Valle, S. Fernández de Mattos, P. Roca, J. Oliver, Hydrogen peroxide regulates the mitochondrial content of uncoupling protein 5 in colon cancer cells, Cell. Physiol. Biochem. 24 (2009) 379–390, https://doi.org/10.1159/000257430.
[60] T. Nakase, Y. Yoshida, K. Nagata, Amplified expression of uncoupling proteins in human brain ischemic lesions, Neuropathology. 27 (2007) 442–447, https://doi.org/10.1111/j.1440-1789.2007.00815.x.
[61] O. Kabil, R. Banerjee, Enzymology of H2S biogenesis, decay and signaling, Antioxid. Redox Signal. 20 (2014) 770–782, https://doi.org/10.1089/ars.2013.5339.
[62] J. Bełtowski, Hydrogen sulfide in pharmacology and medicine—an update, Pharmacol. Rep. 67 (2015) 647–658, https://doi.org/10.1016/j.pharep.2015.01.005.
[63] M. Goubern, M. Andriamihaja, T. Nübel, F. Blachier, F. Bouillaud, Sulfide, the first inorganic substrate for human cells, FASEB J. 21 (2007) 1699–1706, https://doi.org/10.1096/fj.06-7407com.
[64] M. Ackermann, M. Kubitza, K. Maier, A. Brawanski, G. Hauska, A.L. Piña, The vertebrate homolog of sulfide-quinone reductase is expressed in mitochondria of neuronal tissues, Neuroscience. 199 (2011) 1–12, https://doi.org/10.1016/j.neuroscience.2011.10.044.
[65] V. Vitvitsky, O. Kabil, R. Banerjee, High turnover rates for hydrogen sulfide allow for rapid regulation of its tissue concentrations, Antioxid. Redox Signal. 17 (2012) 22–31, https://doi.org/10.1089/ars.2011.4310.
[66] M. Aminlari, A. Malekhusseini, F. Akrami, H. Ebrahimnejad, Cyanide-metabolizing enzyme rhodanese in human tissues: comparison with domestic animals, Comp. Clin. Pathol. 16 (2007) 47–51, https://doi.org/10.1007/s00580-006-0647-x.
[67] W.H. Woo, H. Yang, K.P. Wong, B. Halliwell, Sulphite oxidase gene expression in human brain and in other human and rat tissues, Biochem. Biophys. Res. Commun. 305 (2003) 619–623, https://doi.org/10.1016/S0006-291X(03)00833-7.
[68] Z.-Z. Xie, Y. Liu, J.-S. Bian, Hydrogen sulfide and cellular redox homeostasis, Oxidative Med. Cell. Longev. 2016 (2016) 6043038, https://doi.org/10.1155/2016/6043038.
[69] U. Shefa, M.-S. Kim, N.Y. Jeong, J. Jung, Antioxidant and cell-signaling functions of hydrogen sulfide in the central nervous system, Oxidative Med. Cell. Longev. 2018 (2018) 1873962, https://doi.org/10.1155/2018/1873962.
[70] T. Morikawa, M. Kajimura, T. Nakamura, T. Hishiki, T. Nakanishi, Y. Yukutake, Y. Nagahata, M. Ishikawa, K. Hattori, T. Takenouchi, T. Takahashi, I. Ishii, K. Matsubara, Y. Kabe, S. Uchiyama, E. Nagata, M.M. Gadalla, S.H. Snyder, M. Suematsu, Hypoxic regulation of the cerebral microcirculation is mediated by a carbon monoxide-sensitive hydrogen sulfide pathway, Proc. Natl. Acad. Sci. U. S. A. 109 (2012) 1293–1298, https://doi.org/10.1073/pnas.1119658109.